Int. J. Heat Mass Transfer. Vol. 24, No. 9, pp. 1513–1529, 1981.
Printed in Great Britain

0017-9310/81/091513-17 $02.00/0

FREE SURFACE CONVECTION IN A BOUNDED CYLINDRICAL GEOMETRY

J. S. VRENTAS, R. NARAYANAN and S. S. AGRAWAL
Department of Chemical Engineering, Illinois Institute of Technology, Chicago, IL 60616, U.S.A.

(*Received* 10 *September* 1980 *and in revised form* 25 *February* 1981)

Abstract—Surface tension-driven convection and buoyancy-driven convection in a bounded cylindrical geometry with a free surface are studied for a range of aspect ratios and Nusselt numbers. Linear theory and some aspects of a nonlinear analysis are utilized to determine the critical Marangoni and Rayleigh numbers, the structure of the convective motion, the direction of flow, and the nature of the bifurcation branching. The analysis is based on a somewhat different method for treating free convection problems, the use of Green's functions to reduce the problem to the solution of an integral equation.

NOMENCLATURE

A_m, coefficient in stream function expansion;
B_{np}, coefficient matrix in equation (53);
E, heat transfer enhancement;
E_m, coefficient in stream function expansion;
F_m, coefficient in stream function expansion;
f_m, defined by equation (27);
G_n, defined by equations (39)–(42);
g, Green's function;
$\bar{g}$, magnitude of acceleration of gravity;
H_m, defined by equation (26);
h, heat transfer coefficient at free surface;
I_n, modified Bessel function of first kind of order n;
J_n, Bessel function of first kind of order n;
k, thermal conductivity of liquid;
L, height of liquid;
Ma, Marangoni number $= -\dfrac{(\partial\sigma/\partial T)(\bar{T}-T_a)L}{\mu\kappa}$;
$(Ma)_0$, $(Ma)_1$, coefficients in perturbation series for Ma;
$\overline{(Ma)}_0$, defined by equation (94);
Nu, Nusselt number $= hL/k$;
N_m, defined by equation (28);
p_m, defined by equation (24);
R, radius of cylinder;
Ra, Rayleigh number $= L^3\alpha(\bar{T}-T_a)\bar{g}/\nu\kappa$;
$(Ra)_0$, $(Ra)_1$, $(Ra)_2$, coefficients in perturbation series for Ra;
$\overline{(Ra)}_0$, defined by equation (95);
r, radial distance/R;
T^*, temperature;
T, $T^* - \bar{T}/T_a - \bar{T}$;
T_a, temperature of gas;
T_c, conduction temperature distribution;
$\bar{T}$, temperature at bottom surface of cylinder;
T_m, defined by equation (19);
T_{m0}, defined by equation (50);
T_{m1}, defined by equation (51);
T_{n0}^m, eigenfunctions of linear operator;
t, (time) κ/R^2;
U, (axial velocity) L/κ;
V, (radial velocity) L/κ;
Y_m, defined by equations (29) and (30);
z, axial distance/R.

Greek symbols

α, thermal coefficient of expansion;
α_m, roots of equation (20);
β, L/R;
δ, Dirac delta function;
ε, perturbation parameter;
θ, dimensionless deviation temperature;
θ_0, θ_1, zero-and first-order terms of perturbation series for θ;
κ, thermal diffusivity of liquid;
λ_n, λ_n^m, eigenvalues of linear operator;
μ, viscosity of liquid;
ν, kinematic viscosity of liquid;
σ, surface tension;
ψ, dimensionless stream function;
ψ_0, ψ for θ_0 and $Ma = 1$ or $Ra = 1$;
ψ_1, ψ for θ_1 and $Ma = 1$ or $Ra = 1$;
ω, dimensionless vorticity.

INTRODUCTION

A LARGE number of theoretical and experimental investigations have been concerned with the study of thermal convection in heated horizontal fluid layers. Comprehensive surveys of past work have been given by Chandrasekhar [1], Koschmieder [2], Palm [3] and Rogers [4]. Most of the early theoretical studies dealt with the linear theory of fluid layers of infinite horizontal extent. Rayleigh [5], Jeffreys [6–8], Low [9], Pellew and Southwell [10], and Reid and Harris [11] made important contributions to the linear theory of buoyancy-driven convection, whereas Pearson [12], Scriven and Sternling [13], Nield [14, 15],

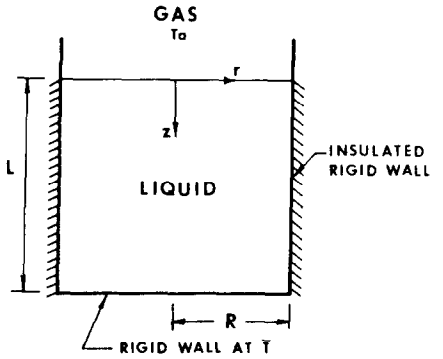

FIG. 1. Schematic of physical system.

Smith [16], Berg and Acrivos [17] and Zeren and Reynolds [18] considered linearized cellular convection for which surface tension gradients were at least partially responsible for the fluid motion. The nonlinear theory of cellular convection in infinite layers has also received considerable attention. The papers of Malkus and Veronis [19], Schlüter, Lortz and Busse [20], Scanlon and Segel [21], Joseph and Shir [22], and Kraska and Sani [23] are representative of the type of work done in this area.

Unfortunately, the results from the convective theory of infinite layers are not completely satisfactory from several points of view. First, the eigenvalue problem in infinite layers can lead to eigenvalues which have an infinite multiplicity. Hence, there can exist an infinite number of possible flow patterns for the linear solution associated with each eigenvalue, and this behavior persists for finite amplitude solutions to the equations of change [19]. Consequently, an infinite layer analysis does not yield a definitive conclusion as to the pattern of the motion for a particular set of conditions. Second, it is not always easy to make a connection between experiments and the predictions of infinite layer theory. The experimentalist of course seeks to approximate an infinite layer by utilizing a bounded geometry with horizontal dimensions which are much larger than the fluid depth. However, it may not be possible to effectively eliminate all of the effects of the lateral boundaries which of course are not considered in the theory for infinite layers. In addition, it may not be easy to minimize temperature variations over a large surface area. Finally, the eigenvalue problem which describes the bounded experimental approximation to an infinite layer very probably has simple eigenvalues, and the distance between successive eigenvalues decreases as the size of the domain increases [24]. Thus, although it is possible to estimate experimentally the dimensionless critical temperature difference at the onset of convection, the crowding of the eigenvalues makes it difficult to study the characteristics of the supercritical convection. This spectral crowding leads to closely bunched solution branches for the various eigenvalues, and the inevitable thermal fluctuations present in physical systems make it quite possible that several solution branches may be unknowingly observed in the same experiment.

As a consequence of the above difficulties with the infinite layer theory, attention has been focused recently on the analysis of thermal convection in geometries which have at least one bounded horizontal dimension. Both linear and nonlinear buoyancy-driven convection in domains bounded by rigid walls have been investigated [25–41], and a number of investigators [24, 27, 33, 42, 43] have considered density-driven convection in bounded regions with at least one free surface. The free surfaces for this latter set of investigations were chosen primarily for mathematical simplicity, and we believe it is fair to say that none of the configurations examined in these papers is readily realizable in the laboratory. Furthermore, no comprehensive study of surface tension-driven convection in a bounded region appears to be available at this time.

The principal objective of this investigation is thus the analysis of both buoyancy-driven and surface tension-driven cellular convection in a bounded, free surface configuration which can be readily examined experimentally. We consider thermal convection in a liquid layer contained in a vertical circular cylinder with a single free boundary, the top surface, which is in contact with an inviscid gas phase. A second objective of this study is the development of a somewhat different method for analyzing free convection problems. This method involves the use of Green's functions to reduce the problem to the solution of an integral equation.

In this paper, we develop linear, steady solutions of this free convection problem for the case when the motion is driven solely by surface tension gradients, and the same program is carried out for the case when only the buoyancy mechanism for convection is operative. In a later paper, the theory of differential operators is used to investigate the linearized stability of these problems, and some aspects of combined buoyancy and surface tension mechanisms are examined. Furthermore, we later consider steady, nonlinear solutions for both buoyancy-and surface tension-driven cellular convection.

FORMULATION OF PROBLEM

The geometrical configuration considered in this study is depicted in Fig. 1. Thermal convection for this system is analyzed subject to the following assumptions

(a) the gas phase is inviscid and the liquid phase is a one-component Newtonian fluid;
(b) the surface phase is an ideal surface fluid with mechanical properties determined solely by the surface tension;
(c) all physical properties with the exception of density and surface tension are constant;
(d) there is no mass transfer between the gas and liquid

phases;
(e) viscous dissipation is negligible;
(f) the standard Boussinesq approximation is introduced so that the surface tension and the density in the body force term are linear functions of temperature;
(g) the Prandtl number of the liquid is infinite;
(h) the surface tension is sufficiently high so that deformation of the free surface is negligible, and it is possible to assume that the interface is effectively flat;
(i) the velocity and temperature fields are axisymmetric.

Since the first six assumptions are standard and can usually be adequately approximated in the laboratory, we consider justification of the remaining three assumptions. Experience with natural convection problems (for example, see Liang, Vidal and Acrivos [33]) indicates that infinite Prandtl number solutions are good approximations to the convective motion for Prandtl numbers greater than about 5. Many common liquids fall in this range, and experiments are frequently conducted with fluids which have Prandtl numbers in the 100–1000 range. The infinite Prandtl number assumption serves to linearize the equations of motion and allows the development of a solution method which involves deriving an integral equation for the temperature field.

The assumption of a flat interface, which is valid in the limit of zero crispation number [13], will lead to erroneous predictions for very thin layers of very viscous fluids. However, there appears to be a large class of important convection problems for which the approximation of a zero crispation number is adequate. For example, crispation numbers for the important experiments of Koschmieder [44] and of Hoard, Robertson and Acrivos [45] were less than 10^{-4}. In addition, Palmer and Berg [46] concluded that deformability of the free surface played an insignificant role in their stability experiments with heated liquid pools.

The critical assumption is of course that of axisymmetric velocity and temperature fields. Ever since the classic experimental work of Bénard [47], it has been assumed that convection in a liquid layer which is heated from below and cooled by an air surface will lead to a pattern of hexagonal cells rather than to an axisymmetric circular roll cell pattern. However, subsequent work has cast some doubt on the general validity of this conclusion. The infinite layer stability analysis of Schlüter, Lortz and Busse [20] shows that two-dimensional rolls are the only stable convective pattern for buoyancy-driven convection for fluids with temperature independent physical properties. Furthermore, Hoard, Robertson and Acrivos [45], using a fluid with a highly temperature dependent viscosity, observed a roll pattern for sufficiently deep fluid layers. These investigators argued that surface contamination in this experiment made it quite likely that the motion was due to buoyancy forces alone. Hence, it is reasonable to conclude that axisymmetric patterns are important for free surface convection dominated by buoyancy effects. On the other hand, the infinite layer stability analyses of Scanlon and Segel [21] and Kraska and Sani [23] indicate that hexagons are the preferred convective state in the vicinity of the critical point for cellular motion with surface tension gradients. Furthermore, Koschmieder [44] and Hoard, Robertson and Acrivos [45] observed motion of the hexagonal type for sufficiently supercritical convection under an air surface under conditions for which surface tension effects are important. However, Koschmieder also reported a stable ring pattern at a lower temperature difference, and Liang, Vidal and Acrivos [33] observed stable roll cells for convection with a free upper surface. Consequently, the possibility of an axisymmetric flow pattern can not be discounted even when significant surface tension effects are present. Furthermore, it is reasonable to expect that the shape of the lateral walls will increasingly influence the geometry of the convection cells as the radius to height ratio of the container decreases, and a pattern of hexagons may well give way to circular rolls for sufficiently small values of R/L. Indeed, two experiments of Hoard, Robertson and Acrivos [45] appear to support this contention.

With the introduction of the assumption of axial symmetry, it is convenient to cast the equations of motion into a stream function-vorticity form. The dimensionless vorticity transport equation can be written as

$$\frac{\partial^2\omega}{\partial r^2}+\frac{1}{r}\frac{\partial\omega}{\partial r}-\frac{\omega}{r^2}+\frac{\partial^2\omega}{\partial z^2}=\frac{Ra}{\beta}\frac{\partial T}{\partial r} \tag{1}$$

$$\omega=\beta\left(\frac{\partial V}{\partial z}-\frac{\partial U}{\partial r}\right) \tag{2}$$

and the dimensionless equation for stream function takes the form

$$\frac{\partial^2\psi}{\partial r^2}-\frac{1}{r}\frac{\partial\psi}{\partial r}+\frac{\partial^2\psi}{\partial z^2}=\frac{\omega r}{\beta^3} \tag{3}$$

$$U=-\frac{\beta^2}{r}\frac{\partial\psi}{\partial r} \tag{4}$$

$$V=\frac{\beta^2}{r}\frac{\partial\psi}{\partial z}. \tag{5}$$

These equations describe both steady and unsteady velocity fields at the infinite Prandtl number limit. The boundary conditions for vorticity can be written as

$$\omega=0,\quad r=0,\quad 0<z<\beta \tag{6}$$

$$\omega=k_1(z),\quad r=1,\quad 0<z<\beta \tag{7}$$

$$\omega=k_2(r),\quad z=0,\quad 0<r<1 \tag{8}$$

$$\omega=k_3(r),\quad z=\beta,\quad 0<r<1 \tag{9}$$

where $k_1(z)$, $k_2(r)$ and $k_3(r)$ are unknown vorticity distributions on the bounding surfaces of the container. The stream function boundary conditions can be expressed as follows:

$$\psi = 0, \quad \frac{1}{r}\frac{\partial \psi}{\partial r} = \frac{\partial^2 \psi}{\partial r^2}, \quad r=0, \quad 0<z<\beta \tag{10}$$

$$\psi = 0, \quad \frac{\partial \psi}{\partial r} = 0, \quad r=1, \quad 0<z<\beta \tag{11}$$

$$\psi = 0, \quad \frac{1}{r}\frac{\partial^2 \psi}{\partial z^2} = -\frac{Ma}{\beta^2}\frac{\partial T}{\partial r}, \quad z=0, \quad 0<r<1 \tag{12}$$

$$\psi = 0, \quad \frac{\partial \psi}{\partial z} = 0, \quad z=\beta, \quad 0<r<1. \tag{13}$$

The unsteady energy equation for this problem takes the form

$$\frac{\partial T}{\partial t} + \frac{\beta}{r}\left[\frac{\partial \psi}{\partial z}\frac{\partial T}{\partial r} - \frac{\partial \psi}{\partial r}\frac{\partial T}{\partial z}\right] = \frac{\partial^2 T}{\partial r^2} + \frac{1}{r}\frac{\partial T}{\partial r} + \frac{\partial^2 T}{\partial z^2} \tag{14}$$

and steady solutions to this equation will be obtained subject to the following boundary conditions

$$\frac{\partial T}{\partial r} = 0, \quad r=0, \quad 0<z<\beta \tag{15}$$

$$\frac{\partial T}{\partial r} = 0, \quad r=1, \quad 0<z<\beta \tag{16}$$

$$\frac{\partial T}{\partial z} = \frac{Nu}{\beta}(T-1), \quad z=0, \quad 0<r<1 \tag{17}$$

$$T = 0, \quad z=\beta, \quad 0<r<1. \tag{18}$$

Clearly the nonlinearity of the problem is concentrated in the convective terms of the energy equation.

Although these equations can of course be used to consider convection with combined buoyancy and surface tension effects, we shall be primarily interested in the two extreme cases: surface tension-driven convection in the absence of buoyancy (the Marangoni problem) and buoyancy-driven convection with no surface tension effects (the Rayleigh problem).

SOLUTION FOR THE STREAM FUNCTION

Since the boundary conditions for most cellular convection problems preclude the possibility of using a strict separation of variables approach, the usual practice [28, 31, 37, 38] in solving for the velocity and temperature fields in bounded geometries is to choose trial functions which satisfy the boundary conditions and then to minimize the errors in the bulk equations of change in an appropriate manner. We prefer to solve for ω and ψ by using a method [48] which parallels the separation of variables approach. Exact solutions are obtained to the partial differential equations for ω and ψ, and the constants in the eigenfunction expansions are determined by satisfying the boundary conditions. However, since series of nonorthogonal functions are involved in this method, it is necessary to solve an infinite system of linear algebraic equations to determine all of these constants. In the usual separation of variables technique, simultaneous determination of the eigenfunction coefficients is usually avoided owing to the orthogonality of the eigenfunctions.

If we expand the radial temperature derivative in equation (1) in a Fourier–Bessel series of the form

$$\frac{\partial T}{\partial r} = \sum_{m=1}^{\infty} T_m(z)\, J_1(\alpha_m r) \tag{19}$$

with the α_m given by

$$J_1(\alpha_m) = 0 \tag{20}$$

then it is easy to obtain the following solution to the vorticity equation

$$\omega = 2\sum_{m=1}^{\infty} J_1(\alpha_m r)\sinh\left[\alpha_m(z-\beta)\right]\{Q_m^1(z) + B_m\} + 2\sum_{m=1}^{\infty} J_1(\alpha_m r)\sinh(\alpha_m z)\{Q_m^2(z) + C_m\} + \sum_{m=1}^{\infty} D_m I_1\left(\frac{m\pi r}{\beta}\right)\sin\left(\frac{m\pi z}{\beta}\right) \tag{21}$$

$$Q_m^1 = p_m \int_0^z \sinh(\alpha_m \xi)\, T_m(\xi)\, d\xi \tag{22}$$

$$Q_m^2 = p_m \int_z^\beta \sinh\left[\alpha_m(\xi-\beta)\right] T_m(\xi)\, d\xi \tag{23}$$

$$p_m = \frac{Ra}{2\alpha_m \beta \sinh(\alpha_m \beta)}. \tag{24}$$

This solution contains three undetermined infinite sets of coefficients: B_m, C_m and D_m. Utilization of this expression for ω in equation (3) and solution of this second-order equation yield the following equation for the stream function

$$\psi = \sum_{m=1}^{\infty} rJ_1(\alpha_m r)\left[H_m(z) + N_m(z)\right] + \sum_{m=1}^{\infty} A_m f_m(r)\sin\left(\frac{m\pi z}{\beta}\right) \tag{25}$$

where

$$H_m(z) = 2F_m\left[\left(1-\frac{z}{\beta}\right)\sinh(\alpha_m z)\right] + 2E_m\left[z\sinh\alpha_m(z-\beta)\right] \tag{26}$$

$$f_m(r) = rI_1\left(\frac{m\pi r}{\beta}\right)I_2\left(\frac{m\pi}{\beta}\right) - r^2 I_2\left(\frac{m\pi r}{\beta}\right)I_1\left(\frac{m\pi}{\beta}\right)\Big/ I_2^2\left(\frac{m\pi}{\beta}\right) \tag{27}$$

$$N_m(z) = \int_0^\beta Y_m(z|\xi)\, T_m(\xi)\, d\xi \tag{28}$$

$$Y_m(z|\xi) = \frac{p_m}{\alpha_m \beta^3}\left\{\frac{(z-\beta)\sinh(\alpha_m z)\sinh(\alpha_m \xi)}{\sinh(\alpha_m \beta)} - \frac{z\sinh\left[\alpha_m(z-\beta)\right]\sinh(\alpha_m \xi)\cosh(\alpha_m \beta)}{\sinh(\alpha_m \beta)} + \frac{\left[\xi\alpha_m\cosh(\alpha_m \xi) - \sinh(\alpha_m \xi)\right]\sinh\left[\alpha_m(z-\beta)\right]}{\alpha_m}\right\} = a_m(z,\xi) \quad \xi < z \leqq \beta \tag{29}$$

$$Y_m(z|\xi) = a_m(\xi, z) \quad 0 \leqq z < \xi. \tag{30}$$

The three sets of coefficients are now A_m, E_m and F_m, and these constants are determined by requiring that the derivative boundary conditions for the stream function are satisfied on $r = 1$, $z = 0$ and $z = \beta$. Utilization of a standard Fourier coefficient approach yields infinite systems of equations for the three infinite sets of coefficients. Explicit forms of these equations and the solution method for the constants A_m, E_m and F_m for a given temperature field are given elsewhere [49]. The above set of equations represents a straightforward method for calculating ψ for a known temperature field, and the equations are valid for both steady and unsteady temperature fields and for linearized and finite amplitude or nonlinear solutions to the temperature equation.

SOLUTION FOR THE TEMPERATURE FIELD

We now seek steady solutions to the energy equation since there is reason to believe that steady rather than time periodic solutions exist near the critical point. Although this assertion has not yet been proved generally for surface tension-driven convection, Vidal and Acrivos [50] have carried out calculations which show that there is stationary rather than oscillatory motion at the onset of convection for the Marangoni problem in infinite layers. Since the nonlinearity in equation (14) is concentrated in the convective terms, it proves convenient to treat these terms as a nonhomogeneous part of the equation for T and solve the steady form of the energy equation using the method of Green's functions. The solution of the steady form of equation (14) subject to equations (15)–(18) can thus be written as

$$T = \beta \int_0^\beta \int_0^1 g \frac{\partial \psi}{\partial r_0} \frac{\partial T}{\partial z_0} \mathrm{d}r_0 \, \mathrm{d}z_0 - \beta \int_0^\beta \int_0^1 g \frac{\partial \psi}{\partial z_0} \frac{\partial T}{\partial r_0} \mathrm{d}r_0 \, \mathrm{d}z_0 + T_c \tag{31}$$

where T_c is the conduction solution

$$T_c = \frac{Nu}{1+Nu}\left(1 - \frac{z}{\beta}\right) \tag{32}$$

and $g(r, z|r_0, z_0)$ is the Green's function solution of the following problem

$$\nabla^2 g = -\frac{\delta(r-r_0)\,\delta(z-z_0)}{r} \tag{33}$$

$$\frac{\partial g}{\partial r} = 0, \quad r = 0 \tag{34}$$

$$\frac{\partial g}{\partial r} = 0, \quad r = 1 \tag{35}$$

$$\frac{\partial g}{\partial z} - \frac{Nu}{\beta} g = 0, \quad z = 0 \tag{36}$$

$$g = 0, \quad z = \beta. \tag{37}$$

The Green's function g can be expressed as

$$g(r, z|r_0, z_0) = G_0(z|z_0) - 2 \sum_{n=1}^{\infty} \frac{J_0(\alpha_n r_0)\, J_0(\alpha_n r)\, G_n(z|z_0)}{J_0^2(\alpha_n)} \tag{38}$$

where

$$G_0(z|z_0) = \frac{2\beta[1 + (Nuz/\beta)][1 - (z_0/\beta)]}{1 + Nu} = b_0(z, z_0), \; 0 \leqq z < z_0 \tag{39}$$

$$G_0(z|z_0) = b_0(z_0, z), \quad z_0 < z \leqq \beta \tag{40}$$

and, for $n \geqq 1$

$$G_n(z|z_0) = [\alpha_n\beta \cosh(\alpha_n z) + Nu \sinh(\alpha_n z)] \times \frac{[\cosh(\alpha_n\beta)\sinh(\alpha_n z_0) - \sinh(\alpha_n\beta)\cosh(\alpha_n z_0)]}{\alpha_n[\alpha_n\beta\cosh(\alpha_n\beta) + Nu\sinh(\alpha_n\beta)]} = b_n(z, z_0), \quad 0 \leqq z < z_0 \tag{41}$$

$$G_n(z|z_0) = b_n(z_0, z), \quad z_0 < z \leqq \beta. \tag{42}$$

Since an explicit expression has been derived for ψ in terms of the temperature field, equation (31) can be regarded as a nonlinear integral equation (strictly, a nonlinear integro-differential equation) for the temperature. It proves convenient to express the temperature as

$$T(r, z) = T_c(z) + \theta(r, z) \tag{43}$$

where θ is the temperature deviation from the conduction solution. Thus, equation (31) becomes

$$\theta = -\frac{Nu}{1+Nu} \int_0^\beta \int_0^1 g \frac{\partial \psi}{\partial r_0} \mathrm{d}r_0 \, \mathrm{d}z_0 + \beta \int_0^\beta \int_0^1 g \left[\frac{\partial \psi}{\partial r_0}\frac{\partial \theta}{\partial z_0} - \frac{\partial \psi}{\partial z_0}\frac{\partial \theta}{\partial r_0}\right] \mathrm{d}r_0 \, \mathrm{d}z_0 \tag{44}$$

and this equation provides the vehicle for the calculation of the temperature field for both linear and nonlinear problems.

LINEAR MARANGONI PROBLEM

We seek a solution to the Marangoni problem ($Ra = 0$) valid in the neighborhood of the critical point by postulating series for θ and Ma of the form

$$\theta = \varepsilon\theta_0 + \varepsilon^2\theta_1 + \ldots \tag{45}$$

$$Ma = (Ma)_0 + \varepsilon(Ma)_1 + \ldots \tag{46}$$

where the perturbation parameter ε is some convenient measure of the amplitude of the convective solution. A definition of ε which is useful for the present investigation is given later. Since ψ is a linear functional of the temperature field, it can be easily shown that

$$\psi = \varepsilon(Ma)_0\psi_0 + \varepsilon^2[(Ma)_0\psi_1 + (Ma)_1\psi_0] + \ldots \tag{47}$$

where ψ_0 and ψ_1 are stream functions for the temperature fields θ_0 and θ_1, respectively, with $Ma = 1$. Substitution of equations (45) and (47) into equation (44) yields the following two equations for θ_0 and θ_1

$$\frac{\theta_0}{(Ma)_0} = -\frac{Nu}{1+Nu}\int_0^\beta\int_0^1 g\frac{\partial\psi_0}{\partial r_0}\,dr_0\,dz_0 \quad (48)$$

$$\frac{\theta_1}{(Ma)_0} = -\frac{Nu}{1+Nu}\int_0^\beta\int_0^1 g\frac{\partial\psi_1}{\partial r_0}\,dr_0\,dz_0 - \frac{Nu}{1+Nu}\int_0^\beta\int_0^1 g\frac{(Ma)_1}{(Ma)_0}\frac{\partial\psi_0}{\partial r_0}\,dr_0\,dz_0 + \beta\int_0^\beta\int_0^1 g\left[\frac{\partial\psi_0}{\partial r_0}\frac{\partial\theta_0}{\partial z_0} - \frac{\partial\psi_0}{\partial z_0}\frac{\partial\theta_0}{\partial r_0}\right]dr_0\,dz_0. \quad (49)$$

It is convenient at this point to introduce the following series expansions for θ_0 and θ_1

$$\theta_0 = T_{00}(z) - \sum_{m=1}^{\infty}\frac{T_{m0}(z)}{\alpha_m}J_0(\alpha_m r) \quad (50)$$

$$\theta_1 = T_{01}(z) - \sum_{m=1}^{\infty}\frac{T_{m1}(z)}{\alpha_m}J_0(\alpha_m r). \quad (51)$$

Utilization of equations (38) and (50) and the derived expression for the stream function in equation (48) produces the following system of equations

$$T_{00} = 0 \quad (52)$$

$$\frac{T_{n0}(0)}{(Ma)_0} = \frac{\alpha_n^2 Nu}{1+Nu}\sum_{p=1}^{\infty}B_{np}T_{p0}(0), \quad n\geqq 1 \quad (53)$$

where the coefficient matrix B_{np} depends only on β and is defined elsewhere [49]. This equation represents an infinite system of linear, homogeneous algebraic equations and is thus an eigenvalue problem for the eigenvalues $1/(Ma)_0$ and the corresponding eigenvectors $T_{n0}(0)$.

If ε is defined by the expression

$$\varepsilon^2 = \sum_{m=0}^{\infty}[T_m(0)]^2 \quad (54)$$

the normalization condition for the eigenvector $T_{m0}(0)$ takes the following form

$$\sum_{m=0}^{\infty}[T_{m0}(0)]^2 = 1. \quad (55)$$

Also, if $(Ma)_1 \neq 0$ and if second- and higher-order terms in ε are neglected, then ε is given by

$$\varepsilon = \frac{Ma-(Ma)_0}{(Ma)_1}. \quad (56)$$

By performing the same operations on equation (49) as were performed on equation (48), we can derive the following equations for the $T_{n1}(0)$

$$T_{01}(0) = (Ma)_0\,\beta\int_0^\beta\int_0^1 G_0(0|z_0)\times\left[\frac{\partial\psi_0}{\partial r_0}\frac{\partial\theta_0}{\partial z_0} - \frac{\partial\psi_0}{\partial z_0}\frac{\partial\theta_0}{\partial r_0}\right]dr_0\,dz_0 \quad (57)$$

$$\frac{T_{n1}(0)}{(Ma)_0} = \frac{\alpha_n^2 Nu}{1+Nu}\sum_{p=1}^{\infty}B_{np}T_{p1}(0) + h_n, \quad n\geqq 1 \quad (58)$$

$$h_n = \frac{(Ma)_1}{(Ma)_0}\bar{j}_n + \bar{k}_n \quad (59)$$

$$\bar{j}_n = -\frac{2\alpha_n Nu}{1+Nu}\int_0^\beta\int_0^1 \times\frac{J_0(\alpha_n r_0)\,G_n(0|z_0)}{J_0^2(\alpha_n)}\frac{\partial\psi_0}{\partial r_0}\,dr_0\,dz_0 \quad (60)$$

$$\bar{k}_n = 2\alpha_n\beta\int_0^\beta\int_0^1\frac{G_n(0|z_0)\,J_0(\alpha_n r_0)}{J_0^2(\alpha_n)} \times\left[\frac{\partial\psi_0}{\partial r_0}\frac{\partial_0}{\partial z_0} - \frac{\partial\psi_0}{\partial z_0}\frac{\partial\theta_0}{\partial r_0}\right]dr_0\,dz_0. \quad (61)$$

Since numerical calculations show that $1/(Ma)_0$ is an algebraically simple eigenvalue of equation (53), then equation (58) will have a solution [51] if, and only if, the single solution, $T^*_{n0}(0)$, of the adjoint homogeneous problem

$$\frac{T^*_{n0}(0)}{(Ma)_0} = \frac{Nu}{1+Nu}\sum_{p=1}^{\infty}\alpha_p^2 B_{pn}T^*_{p0}(0) \quad (62)$$

is orthogonal to the nonhomogeneous vector in equation (58)

$$\sum_{n=1}^{\infty}h_n T^*_{n0}(0) = 0. \quad (63)$$

From this result, we derive the following expression for $(Ma)_1$

$$(Ma)_1 = -\frac{(Ma)_0\sum_{n=1}^{\infty}T^*_{n0}(0)\,\bar{k}_n}{\sum_{n=1}^{\infty}T^*_{n0}(0)\,\bar{j}_n}. \quad (64)$$

Finally, we develop an expression for the heat transfer enhancement, E, which is the ratio of the heat transfer rate from the top surface when cellular convection is present to the heat transfer rate when only the conductive mode is operative

$$E = 1 - \varepsilon^2(1+Nu)\,T_{01}(0) + \ldots, \quad (65)$$

FORMULATION OF LINEAR RAYLEIGH PROBLEM

For the Rayleigh problem ($Ma = 0$), we again are interested in the construction of steady convective solutions. In this case, however, this restriction is totally justified since the possibility of time periodic solutions near the critical point is ruled out owing to the self-adjointness of the linear system for this type of problem [24, 38]. For this problem, we utilize the series expansion given by equation (45) for θ and the following perturbation expansion for Ra near the critical point

$$Ra = (Ra)_0 + \varepsilon(Ra)_1 + \varepsilon^2(Ra)_2 + \ldots. \quad (66)$$

We also have

$$\psi = \varepsilon(Ra)_0 \psi_0 + \varepsilon^2 [(Ra)_0 \psi_1 + (Ra)_1 \psi_0] + \ldots. \quad (67)$$

Here, ψ_0 and ψ_1 are solutions to the stream function equation corresponding to temperature fields θ_0 and θ_1, respectively, with $Ra = 1$.

If we utilize the above perturbation series and proceed as in the derivation for the Marangoni problem, we derive the following results for the $T_{n0}(z)$

$$T_{00} = 0 \quad (68)$$

$$b_n = -\frac{\alpha_n^2 Nu}{1+Nu} \quad (69)$$

$$\frac{T_{n0}(z)}{(Ra)_0} = P_n(z) + b_n \int_0^\beta \Phi_n(z|\xi) \times T_{n0}(\xi)\,d\xi, \quad n \geqq 1. \quad (70)$$

The quantity $P_n(z)$ is defined elsewhere [49] and

$$\Phi_n(z|\xi) = \int_0^\beta G_n(z|z_0)\, Y_n^*(z_0|\xi)\,dz_0 \quad (71)$$

where Y_n^* is the value of Y_n with $Ra = 1$. In this form, equation (70) can be regarded as a linear, non-homogeneous Fredholm integral equation of the second kind for $T_{n0}(z)$. We shall develop a solution for each equation in the infinite system represented by equation (70) in terms of the eigenvalues and eigenfunctions of the linear integral operator K

$$KT_{n0} = \int_0^\beta \Phi_n(z|\xi)\, T_{n0}(\xi)\,d\xi. \quad (72)$$

This task is complicated somewhat by the fact that it is not possible to establish a symmetry property for the kernel $\Phi_n(z|\xi)$.

EIGENVALUES AND EIGENFUNCTIONS OF THE LINEAR INTEGRAL OPERATOR

The eigenvalue problem for the linear integral operator can be posed as

$$KT_{n0} = \lambda_n T_{n0} \quad (73)$$

and this eigenvalue problem can be transformed to the solution of the sixth-order equation with $D = d/dz$

$$(D^2 - \alpha_n^2)^3 T_{n0} = \frac{T_{n0}}{\lambda_n \beta^4} \quad (74)$$

subject to the following boundary conditions

$$\frac{dT_{n0}}{dz} = \frac{Nu}{\beta} T_{n0}, \quad z=0 \quad (75)$$

$$\frac{d^2T_{n0}}{dz^2} = \alpha_n^2 T_{n0}, \quad z=0 \quad (76)$$

$$\frac{d^4T_{n0}}{dz^4} = \alpha_n^4 T_{n0}, \quad z=0 \quad (77)$$

$$T_{n0} = 0, \quad \frac{d^2T_{n0}}{dz^2} = 0, \quad \frac{d^4T_{n0}}{dz^4} = 0, \quad z=\beta. \quad (78)$$

Before we derive expressions for the eigenvalues λ_n and the eigenfunctions T_{n0} for this problem, it is necessary to state two theorems which establish the properties of the λ_n.

Theorem I. The eigenvalues λ_n of the linear operator K are real.

Theorem II. The eigenvalues λ_n obey the inequalities

$$0 > \lambda_n > -\frac{1}{\beta^4 \alpha_n^6}. \quad (79)$$

The proofs of these theorems and further properties of the linear integral operator are considered elsewhere [49].

With the help of theorems I and II, it can be shown that the infinite set of eigenvalues of K, the λ_n^m, are the solutions of the following equation

$$-(\tau_n - \alpha_n^2)^{1/2} \cot[(\tau_n - \alpha_n^2)^{1/2}\beta] = \frac{3Nu}{\beta} + \frac{2(j_n \sinh 2\beta j_n + k_n \sin 2\beta k_n)}{\cosh 2\beta j_n - \cos 2\beta k_n} \quad (80)$$

$$\tau_n = \left(\frac{1}{\beta^4 |\lambda_n|}\right)^{1/3} \quad (81)$$

$$j_n = \left[\frac{(\alpha_n^4 + \tau_n \alpha_n^2 + \tau_n^2)^{1/2}}{2} + \frac{(\alpha_n^2 + \frac{1}{2}\tau_n)}{2}\right]^{1/2} \quad (82)$$

$$k_n = \left[\frac{(\alpha_n^4 + \tau_n \alpha_n^2 + \tau_n^2)^{1/2}}{2} - \frac{(\alpha_n^2 + \frac{1}{2}\tau_n)}{2}\right]^{1/2}. \quad (83)$$

The eigenfunction corresponding to the eigenvalue λ_n^m can be expressed as follows:

$$T_{n0}^m(z) = \sin[(\tau_n^m - \alpha_n^2)^{1/2}(z-\beta)] + E_{nm} \sinh[j_n^m(z-\beta)] \cos[k_n^m(z-\beta)] + F_{nm} \sin[k_n^m(z-\beta)] \cosh[j_n^m(z-\beta)]. \quad (84)$$

Expressions for the coefficients E_{nm} and F_{nm} are given elsewhere [49].

SOLUTION OF LINEAR RAYLEIGH PROBLEM

We proceed to solve the linear Fredholm integral equation in the standard manner [51], using the eigenfunctions and eigenvalues of the linear operator to form expansions for the individual terms of the integral equation. We can form an expansion for $T_{n0}(z)$ in terms of the eigenfunctions of the linear operator

$$T_{n0}(z) = \sum_{m=1}^{\infty} K_{nm}^0 T_{n0}^m(z) \quad (85)$$

and utilization of this expression in equation (70) leads to the result

$$\frac{K_{nm}^0}{(Ra)_0} = b_n \lambda_n^m K_{nm}^0 + \sum_{t=1}^{\infty} \sum_{q=1}^{\infty} \times K_{tq}^0 Q_{nmtq}, \quad n \geqq 1, \; m \geqq 1. \quad (86)$$

Consequently, in the process of solving the non-homogeneous integral equation for T_{n0}, we have

Table 1. $(Ma)_0$ for first bifurcation point

Nu	R/L=0.5	R/L = 1	R/L = 2	R/L = 4	R/L = 8	R/L = 20
0.01	63517.4	16604.5	8548.1	8330.8	8148.5	8092.9
0.10	6993.0	1851.9	970.9	952.4	924.8	925.9
1.00	1417.4	412.0	250.0	241.3	234.4	232.6
10.00	1572.3	637.0	505.1	465.1	457.6	456.6
100.00	8612.9	4315.2	3625.3	3404.9	3352.1	3339.5

generated an infinite system of linear, homogeneous algebraic equations, and, thus, we have an eigenvalue problem for the eigenvalues $1/(Ra)_0$ and the corresponding eigenvectors K^0_{nm}. The Q_{nmtq} depend only on β and are defined elsewhere [49].

As above, we can derive a normalization condition for the eigenvector

$$\sum_{m=1}^{\infty}\sum_{n=1}^{\infty}(K^0_{nm})^2 = 1. \tag{87}$$

Also, since it is well known that $(Ra)_1 = 0$ for this problem [24], we can calculate ε from the expression

$$\varepsilon = \pm\left[\frac{Ra-(Ra)_0}{(Ra)_2}\right]^{1/2} \tag{88}$$

if third- and higher-order terms in ε are neglected. In addition, it can be shown that the $T_{n1}(z)$ are given by the following equations

$$T_{01} = \beta(Ra)_0\int_0^{\beta}\int_0^1 G_0(z|z_0) \times\left[\frac{\partial\psi_0}{\partial r_0}\frac{\partial\theta_0}{\partial z_0} - \frac{\partial\psi_0}{\partial z_0}\frac{\partial\theta_0}{\partial r_0}\right]dr_0\,dz_0 \tag{89}$$

$$T_{n1} = \sum_{m=1}^{\infty} K^1_{nm}\,T^m_{n0} \tag{90}$$

$$\frac{K^1_{nm}}{(Ra)_0} = b_n\lambda_n^m K^1_{nm} + \sum_{t=1}^{\infty}\sum_{q=1}^{\infty} K^1_{tq}\,Q_{nmtq} + C_{nm},\quad n\geqq 1,\ m\geqq 1. \tag{91}$$

The C_{nm}, which are defined elsewhere [49], represent the nonhomogeneous terms of the infinite system of linear algebraic equations for the K^1_{nm}. It is convenient to use the theory of differential operators to derive an expression for $(Ra)_2$. We anticipate a result of a later paper and write

$$\frac{(Ra)_2}{(Ra)_0}\int_0^{\beta}\int_0^1\psi_0\frac{\partial\theta_0}{\partial r}dr\,dz = \frac{\beta(1+Nu)}{Nu}\int_0^{\beta}\int_0^1\left[T_{01} - \sum_{m=1}^{\infty}\sum_{p=1}^{\infty}\frac{Y_{mp}\,T^p_{m0}}{\alpha_m}J_0(\alpha_m r)\right] \times\left[\frac{\partial\psi_0}{\partial r}\frac{\partial\theta_0}{\partial z} - \frac{\partial\psi_0}{\partial z}\frac{\partial\theta_0}{\partial r}\right]dr\,dz \tag{92}$$

where T_{01} is given by equation (89) and Y_{mp} is a particular solution of equation (91).

The integral equation method used to analyze the Rayleigh problem is similar in some respects to a method used by Kirchgässner and Sorger [52] in a branching analysis of the Taylor problem. More details of the mathematical methods used in this paper are provided elsewhere [49, 53].

Table 2. $(Ra)_0$ at first bifurcation point

Nu	R/L=0.5	R/L=1	R/L=2	R/L=4	R/L=8
0.01	1035524.2	157389.2	71959.1	70250.3	68195.9
0.10	112849.8	17224.4	7991.5	7802.7	7560.5
1.00	20630.2	3256.3	1671.7	1599.0	1555.9
10.00	11609.3	2013.2	1230.3	1113.7	1096.5
100.00	10844.2	1958.4	1247.2	1121.9	1105.4

Table 3. $(Ma)_0$ at first bifurcation point for $Nu = 100$

R/L	$(Ma)_0$
1.00	4315.2
1.33	3717.4
1.43	3665.0
1.75	3686.9
2.00	3625.3
2.25	3512.9
2.61	3458.3
3.79	3402.7
4.00	3404.9

Table 4. $(Ra)_0$ at first bifurcation point for $Nu = 100$

R/L	$(Ra)_0$	$(Ra)_0\ \beta^{-4}$
1.00	1958.4	1.9584×10^3
1.33	1288.7	4.0729×10^3
1.43	1244.7	5.1758×10^3
1.75	1218.4	1.1427×10^4
2.00	1247.2	1.9416×10^4
2.25	1213.5	3.1100×10^4
2.61	1152.5	5.3810×10^4
3.79	1124.7	2.3255×10^5
4.00	1121.8	2.8718×10^5

RESULTS AND DISCUSSION

Values of the critical Marangoni and Rayleigh numbers at the first bifurcation point, $(Ma)_0$ and $(Ra)_0$, are presented as functions of Nu and β in Tables 1 and 2, respectively. The simplicity of the eigenvalues implies that they are bifurcation or branch points for the system [51]. At a given value of Nu, there is a general decrease of both $(Ma)_0$ and $(Ra)_0$ with increasing aspect ratio, R/L, and as much as nearly an eight-fold decrease was observed for the cases considered here. This effect is of course expected since the lateral wall can severely inhibit convective motion and thus has a stabilizing effect. The effect of the side wall diminishes with increasing Nusselt number for both Marangoni and Rayleigh problems. These results appear to be the first comprehensive computations for the free surface geometry considered here. Bentwich [54] has presented some very limited results for this problem. However, some severe approximations are introduced into his analysis, and the few results he presents are not generally in agreement with those presented here. Furthermore, his predicted dependence of $(Ra)_0$ on R/L is not physically realistic.

Charlson and Sani [38] observed local maxima in their plot of the critical Rayleigh number versus aspect ratio for buoyancy-driven convection in a rigid-wall cylinder with an insulating side wall. Consequently, additional critical Marangoni numbers and critical Rayleigh numbers were computed at intermediate values of R/L at $Nu = 100$ to ascertain whether the same phenomenon occurred for the free surface problem considered in this investigation. It is evident from Tables 3 and 4 that local maxima are indeed observed when a finer distribution of R/L is studied.

Jennings and Sani [40] have stated that the critical Rayleigh number should be a nonincreasing function of the size of a bounded domain for conducting side walls. This statement is not true for insulating side walls, as is evident from the results of this study presented in Table 4 and from the insulated wall results of Charlson and Sani [38] which are given in Table 5. However, in a later paper, we use the theory of differential operators to show that

Table 5. $(Ra)_0$ for Charlson and Sani [38]

R/L	$(Ra)_0$	$(Ra)_0\ \beta^{-4}$
1.25	1920.83	4.6895×10^3
1.50	1896.13	9.5992×10^3
1.60	1921.99	1.2596×10^4
1.75	1949.86	1.8287×10^4
2.00	1862.27	2.9796×10^4
2.50	1780.81	6.9562×10^4
2.75	1795.17	1.0267×10^5
3.00	1778.25	1.4403×10^5
3.50	1747.24	2.6219×10^5
3.75	1752.90	3.4664×10^5
4.00	1747.95	4.4747×10^5
4.50	1732.93	7.1060×10^5
5.00	1733.78	1.0836×10^6
5.50	1725.30	1.5787×10^6
6.00	1725.98	2.2368×10^6
6.50	1720.72	3.0716×10^6
7.00	1721.36	4.1329×10^6
8.00	1718.39	7.0385×10^6

Table 6. Comparison of bounded geometries with infinite layers

Nu	$(Ma)_0$ for R/L = 20	$(Ma)_0$ for infinite layer
0.01	8092.9	8079.1
0.10	925.9	917.7
1.00	232.6	232.3
10.00	456.6	454.8
100.00	3339.5	3336.9

$$\frac{\partial[(Ra)_0 \beta^{-4}]}{\partial \beta} < 0 \tag{93}$$

for the axisymmetric Rayleigh problems studied by Charlson and Sani and by the present investigators. It is evident from Tables 4 and 5 that the reported eigenvalues of both investigations obey this inequality.

At a given value of R/L (or β), the critical Marangoni number becomes large as $Nu \to 0$ and as $Nu \to \infty$ and achieves a minimum value in the vicinity of $Nu = 1$. As $Nu \to \infty$, the surface temperature becomes effectively uniform, and large temperature differences are needed to promote convective motion. As $Nu \to 0$, a uniform temperature exists in the liquid layer in the conductive state, and, again, a large temperature difference is necessary for cellular convection. We note here that the critical Marangoni number defined in this study, $(Ma)_0$, is related to the dimensionless group which has been used [14] in infinite layer theory, $\overline{(Ma)_0}$, by the following expression

$$(Ma)_0 = \frac{1+Nu}{Nu}\overline{(Ma)_0}. \tag{94}$$

The difference arises because we have defined the Marangoni number using the temperature difference between the bottom surface of the liquid layer and the gas phase, whereas the temperature difference across the liquid layer in the conductive state is used in infinite layer studies. In the infinite layer analyses, a finite value of $\overline{(Ma)_0}$ at $Nu = 0$ and a monotonic increase of $\overline{(Ma)_0}$ with increasing Nusselt number are computed [14]. However, these results are somewhat artificial since a nonzero temperature difference can be maintained across the liquid layer at $Nu = 0$ in the conductive state only if an infinitely large value of $\bar{T} - T_a$ is applied. Although either definition of the Marangoni number can of course be utilized, we believe that the present definition is more useful in arriving at a physical interpretation of the results.

A comparison of the infinite layer results of Nield [14] for $(Ma)_0$ with the results of this study at $R/L = 20$ is given in Table 6. The difference between the two values is less than one per cent in all cases, and the values for $R/L = 20$ are higher than the infinite layer results as expected. Consequently, an aspect ratio of 20, or even 8, is a reasonable approximation to an infinite layer for the purpose of calculating the critical

Table 7. Comparison of bounded geometries with infinite layers

Nu	$\frac{\text{wavelength (average value for R/L = 20)}}{\text{wavelength (infinite layer)}}$
0.01	1.0594
0.10	0.9931
1.00	1.0213
10.00	1.0273
100.00	0.9971

Table 8. Nusselt number dependence of $(Ra)_0$ for infinite layers

Nu	$(Ra)_0$
0.01	67708.4
0.10	7505.9
0.20	4168.7
0.50	2182.3
1.00	1541.2
2.00	1246.9
5.00	1110.6
10.00	1088.4
20.00	1088.1
50.00	1093.6
100.00	1096.8
1000.00	1100.2
10^{10}	1100.7

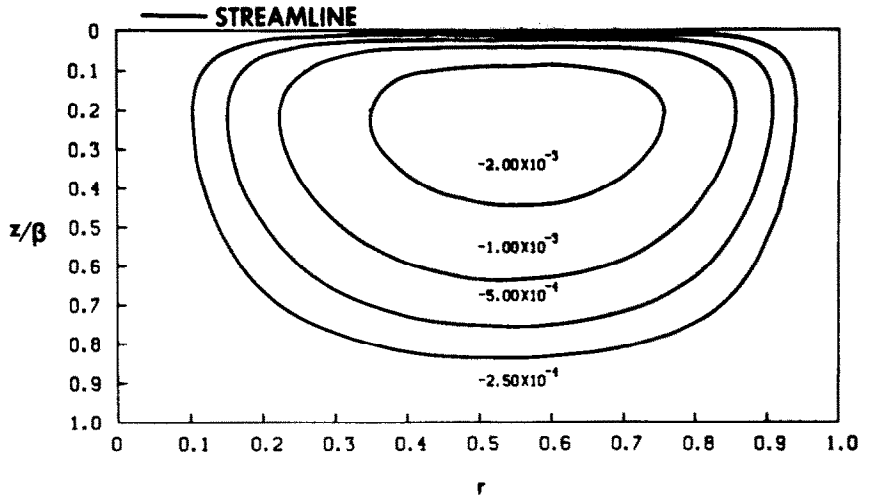

FIG. 2. Streamlines ψ_0 at first bifurcation point for $R/L = 1$ and $Nu = 1$ for $Ra = 0$.

Marangoni number. Really significant increases in $(Ma)_0$ begin to occur when R/L is less than 2. We can also see from Table 7 that there is good agreement between the wavelength from infinite layer theory and an average wavelength (the ratio of the width of a cell to the depth of the fluid layer) computed for a bounded region at $R/L = 20$. Similar results are obtained for the Rayleigh problem.

At a fixed aspect ratio, there is a general decrease of $(Ra)_0$ with increasing Nu. As in the Marangoni problem, large temperature differences are needed to promote convection as $Nu \to 0$. However, large temperature gradients are not necessary as $Nu \to \infty$ since buoyancy-driven convection can of course proceed even if the temperature of the free surface is uniform. It should be noted that there is not a strict decrease of $(Ra)_0$ with increasing Nu at the three highest aspect ratios, $R/L = 2$, 4, and 8, there being a minimum in the $(Ra)_0$ vs Nu curve in the vicinity of $Nu = 10$. We further note that the critical Rayleigh number defined here, $(Ra)_0$, is related to the one used [14] in infinite layer theory, $\overline{(Ra)_0}$, by

$$(Ra)_0 = \frac{1+Nu}{Nu}\overline{(Ra)_0}. \tag{95}$$

The infinite layer analysis [14] shows that $\overline{(Ra)_0}$ increases monotonically with increasing Nu, and we have used the theory of differential operators in a later paper to show that

$$\frac{\partial \overline{(Ra)_0}}{\partial Nu} > 0 \tag{96}$$

for the bounded, axisymmetric flow problem we are considering here. However, the same analysis shows that $\partial(Ra)_0/\partial Nu$ need not have the same sign for all Nu, and a minimum in the $(Ra)_0$ vs Nu curve cannot be excluded. Furthermore, as is evident from Table 8, a

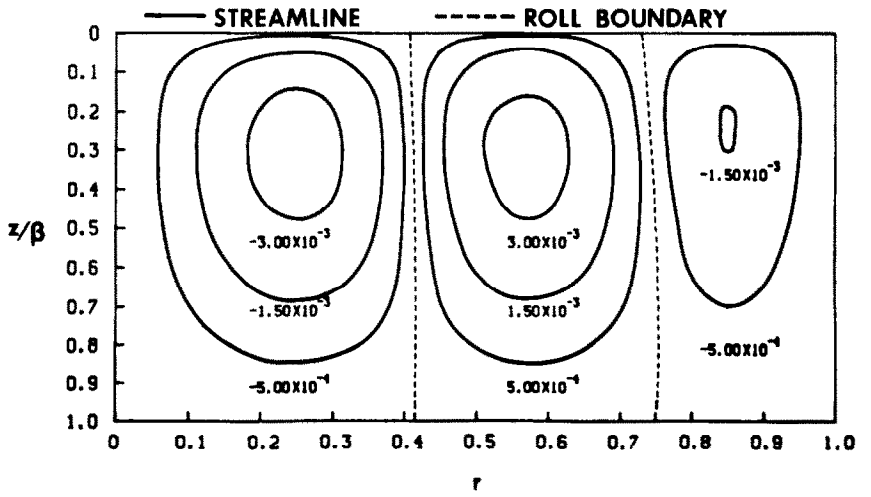

FIG. 3. Streamlines ψ_0 at first bifurcation point for $R/L = 4$ and $Nu = 1$ for $Ra = 0$.

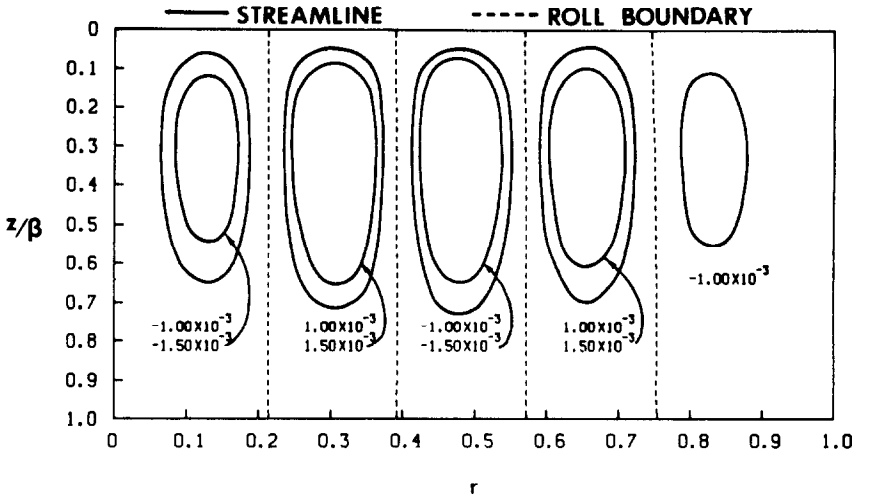

FIG. 4. Streamlines ψ_0 at first bifurcation point for $R/L = 8$ and $Nu = 1$ for $Ra = 0$.

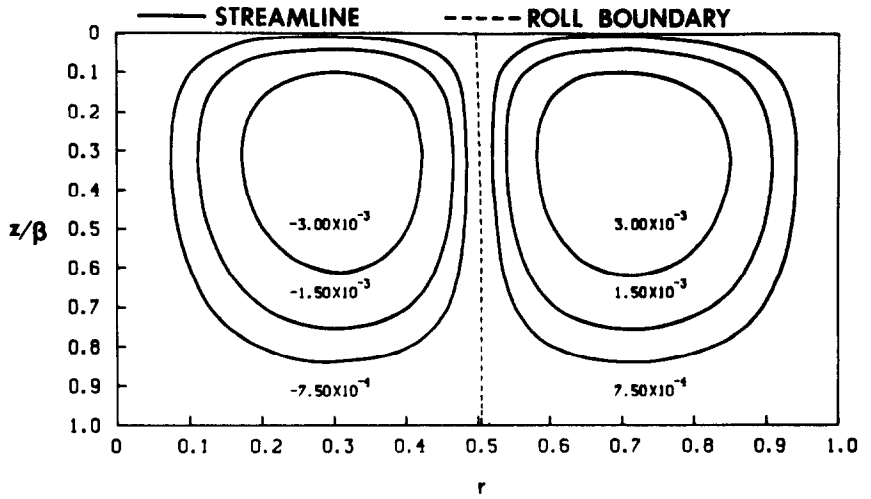

FIG. 5. Streamlines ψ_0 at first bifurcation point for $R/L = 4$ and $Nu = 0.01$ for $Ra = 0$.

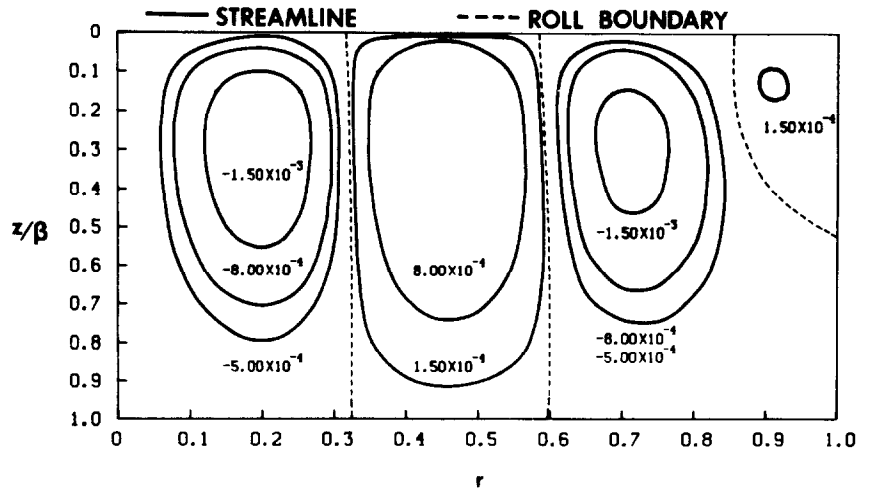

FIG. 6. Streamlines ψ_0 at first bifurcation point for $R/L = 4$ and $Nu = 100$ for $Ra = 0$.

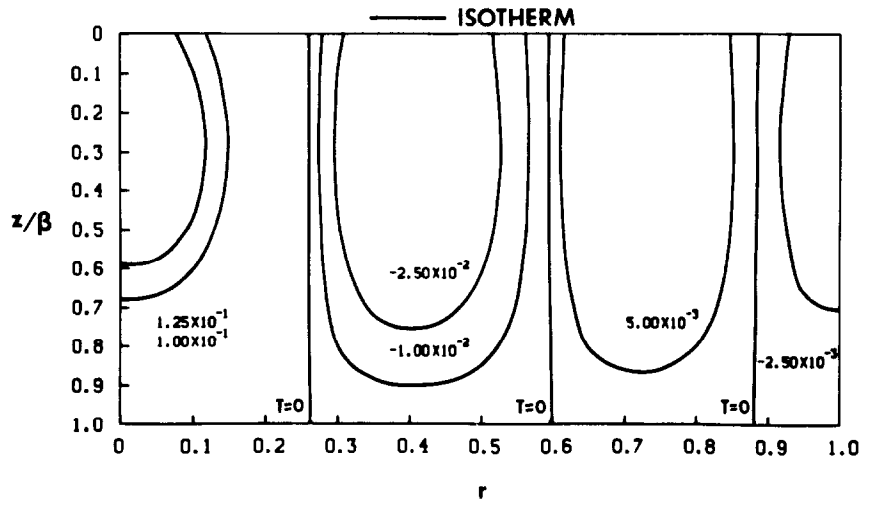

FIG. 7. Isotherms θ_0 at first bifurcation point for $R/L = 4$ and $Nu = 1$ for $Ra = 0$.

minimum exists also in the $(Ra)_0$ vs Nu curve near $Nu = 20$ for the eigenvalues of infinite layer theory.

Streamline plots for ψ_0 at the first bifurcation point for $Ra = 0$, with aspect ratios of 1, 4, and 8 and $Nu = 1$ are presented in Figs. 2–4. We note that the roll cells near the lateral wall are generally weaker, in the sense that convection dies down, than roll cells near the center of the cylinder because of the damping effect of the lateral wall. Figures 3, 5 and 6 show the streamlines for $R/L = 4$ and $Nu = 0.01$, 1, and 100. It is evident that the effect of increasing the Nusselt number is to increase the number of roll cells for a fixed aspect ratio. It will be shown below that this behavior is in evidence for the first bifurcation point for all cases studied in this investigation. Figure 7 shows a typical isotherm plot for the deviation temperature field θ_0 for $R/L = 4$ and $Nu = 1$. It is again evident that the strength of the convection decreases as the wall is approached. In addition, the change of the sign of θ_0 appears to occur reasonably close to the center of a roll cell. Similar results are obtained for $Ma = 0$.

The plots of ψ_0 and θ_0 of course do not give the actual direction or strength of the flow for a roll cell. However, this information can be obtained in the neighborhood of the critical point if computed values of $(Ma)_1$ or $(Ra)_2$ are used to determine single term estimates of ψ and θ. Values of $(Ma)_1$ are presented in Table 9 for some of the cases examined in this investigation. Since $(Ma)_1 > 0$, there exist both supercritical and subcritical steady convective solution branches in the neighborhood of the bifurcation point. The stability of these convective branches in the vicinity of the critical point will be considered later. The possibility of subcritical convective motions for surface tension-driven convection has been suggested by the infinite layer analysis of Davis [55]. The direction of flow on the supercritical side of the bifurcation point at the center of the cylinder is indicated in Table 9. The flow in all of the cases studied is upward at the center of the fluid layer. Liang, Vidal and Acrivos [33] experimentally studied free surface convection in a circular cylinder and reported that the stable flow pattern was an axisymmetric flow field with upward motion near the center of the cell. It is not known how significant surface tension gradients were in producing this flow.

Values of $(Ra)_2$ are presented in Table 10 for some of the cases studied here. Since $(Ra)_1 = 0$, there is no

Table 9. Values of $(Ma)_1$ and direction of flow at center of cylinder

Nu	R/L = 0.5	R/L = 1	R/L = 2	R/L = 4	R/L = 8
0.01	0.29156×10^7 (UP)	0.37385×10^6 (UP)	0.89289×10^5 (UP)	0.28545×10^5 (UP)	0.69800×10^4 (UP)
1.00	0.14749×10^4 (UP)	0.23654×10^3 (UP)	0.85902×10^2 (UP)	0.25073×10^2 (UP)	0.65437×10^1 (UP)
100.00	0.63568×10^5 (UP)	0.30117×10^5 (UP)	0.14353×10^5 (UP)	0.38390×10^4 (UP)	0.87712×10^3 (UP)

Table 10. Values of $(Ra)_2$

Nu	R/L=0.5	R/L=1	R/L=2	R/L=4	R/L=8
0.01	0.78556×10^{10}	0.45397×10^{9}	0.12006×10^{9}	0.46857×10^{8}	0.50900×10^{7}
1.00	0.45882×10^{5}	0.27827×10^{4}	0.80483×10^{3}	0.15436×10^{3}	0.31296×10^{2}
100.00	0.43040×10^{4}	0.30927×10^{3}	0.10118×10^{3}	0.12522×10^{2}	0.25265×10^{1}

Table 11. Critical Marangoni numbers at first four bifurcation points

	Nu = 0.01			Nu = 1.00			Nu = 100.00		
R/L	$\frac{2}{1}$	$\frac{3}{1}$	$\frac{4}{1}$	$\frac{2}{1}$	$\frac{3}{1}$	$\frac{4}{1}$	$\frac{2}{1}$	$\frac{3}{1}$	$\frac{4}{1}$
20	1.00411	1.01397	1.02161	1.00469	1.01036	1.02236	1.00218	1.00621	1.01117
8	1.03139	1.06467	1.17003	1.01898	1.07616	1.11320	1.01412	1.03836	1.06539
4	1.08548	1.38563	1.63311	1.06201	1.23432	1.58988	1.04301	1.14437	1.28180
2	1.53633	2.78888	4.60466	1.33693	2.25789	3.58335	1.16942	1.37876	1.74246
1	2.83316	5.66764	9.42916	2.58063	4.96536	8.11597	1.64552	2.35250	3.09269
0.5	2.96303	5.92876	9.90071	2.81524	5.51827	9.11375	1.76126	2.58157	3.47210

$\frac{2}{1}$, $\frac{3}{1}$, and $\frac{4}{1}$ signify the ratios of the values of $(Ma)_0$ at the second, third, and fourth bifurcation points to $(Ma)_0$ at the first.

Table 12. Critical Rayleigh numbers at first four bifurcation points

	Nu=0.01			Nu=1.00			Nu=100.00		
R/L	$\frac{2}{1}$	$\frac{3}{1}$	$\frac{4}{1}$	$\frac{2}{1}$	$\frac{3}{1}$	$\frac{4}{1}$	$\frac{2}{1}$	$\frac{3}{1}$	$\frac{4}{1}$
8	1.03379	1.06350	1.14210	1.01955	1.07409	1.12547	1.01877	1.06415	1.10390
4	1.06309	1.33467	1.69353	1.07316	1.24327	1.65883	1.10081	1.23916	1.41930
2	1.50255	3.01139	6.03103	1.36023	2.62615	5.19397	1.17579	1.98302	3.72771
1	3.89091	7.68258	10.95412	3.76609	7.63448	10.65388	3.35755	7.82878	9.89159
0.5	2.25637	6.31538	6.69201	2.26798	6.32682	6.69173	2.36894	6.27356	7.02209

$\frac{2}{1}$, $\frac{3}{1}$, and $\frac{4}{1}$ signify the ratios of values of $(Ra)_0$ at the second, third, and fourth bifurcation points to $(Ra)_0$ at the first.

Table 13. Roll cell number at first three bifurcation points ($Ra = 0$)

	Nu = 0.01			Nu = 1.00			Nu = 100.00		
R/L	1	2	3	1	2	3	1	2	3
20	12	13	12	14	15	13	19	19	18
8	5	4	6	5	5	7	8	7	6
4	2	3	4	3	3	4	3	4	3
2	1	2	3	1	2	3	2	1	1
1	1	2	3	1	2	3	1	2	1
0.5	1	2	3	1	2	3	1	2	1

subcritical convection and two supercritical flows are possible in the linear region, one with upflow and the other with downflow at the center of the cylinder.

Critical Marangoni and Rayleigh numbers for the first four bifurcation points are presented in Tables 11 and 12, and the numbers of roll cells for the linear flow fields for the first three bifurcation points are reported in Tables 13 and 14. It is evident that the eigenvalues (critical Marangoni or Rayleigh numbers) crowd together as R/L is increased. This spectral crowding is so severe that there is only approximately a two percent difference between the first and fourth eigenvalues when $R/L = 20$ for the Marangoni problem. From Tables 13 and 14, it is evident, as noted earlier, that the number of roll cells for the first bifurcation point increases with increasing Nusselt number for fixed aspect ratio. Furthermore, the number of radial roll cells increases with increasing aspect ratio at a fixed value of Nu for the first bifurcation point. It is also evident that there is no general pattern in the number of roll cells at the first three bifurcation points for given values of β and Nu for both surface tension and buoyancy problems.

For the first bifurcation point for the Marangoni problem, only radial rolls appear and there is no vertical stacking of the cells. Thus, the number of roll cells alone gives a representative picture of the nature of the cellular motion, with the possible exception of the existence of small corner eddies. However, for higher bifurcation points, vertical stacks of radial rolls are observed, and the roll cell number reported in Table 13 represents the situation near the midpoint of the fluid layer and does not necessarily present a clear picture of the cellular pattern. An example of the vertical stacking of radial rolls at higher bifurcation points for surface tension-driven convection is shown in Fig. 8. For buoyancy-driven convection, there is no vertical stacking of roll cells for the higher bifurcation points, and the number of radial rolls reported in Table 14 thus gives a representative picture of the convective flow pattern.

It is evident from the above results that the solution branches for successive bifurcation points are closely bunched at high aspect ratios, and significantly different convective patterns may be associated with these branches. Thus, it appears preferable to study

Table 14. Roll cell number at first three bifurcation points ($Ma = 0$)

	Nu=0.01			Nu=1.00			Nu=100.00		
R/L	1	2	3	1	2	3	1	2	3
8	5	6	4	6	6	7	7	7	6
4	2	3	4	3	3	4	3	4	2
2	1	2	3	1	2	3	2	2	3
1	1	2	1	1	2	1	1	2	1
0.5	1	1	1	1	1	1	1	1	2

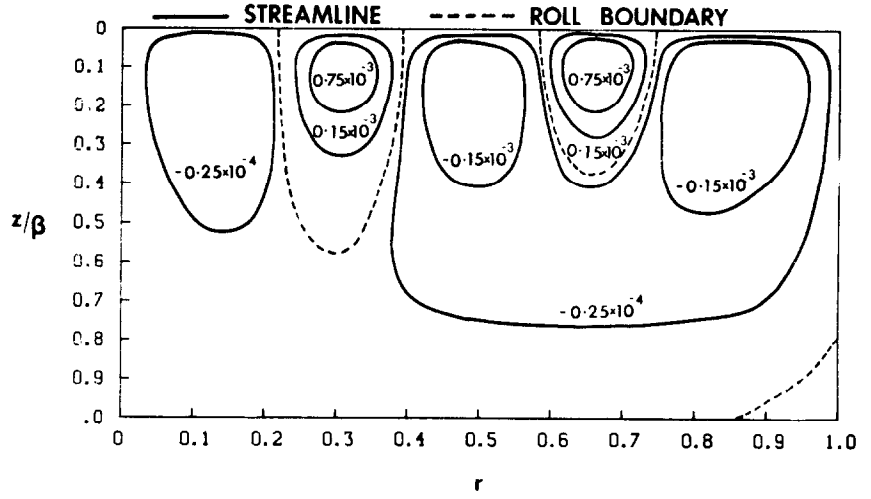

FIG. 8. Streamlines ψ_0 at fifth bifurcation point for $R/L = 2$ and $Nu = 100$ for $Ra = 0$.

cellular convection in geometries with small aspect ratios (less than about 4) to avoid the possibility that more than one solution branch may be observed owing to the inevitable thermal fluctuations present in physical systems.

Finally, although the present analyses of the Marangoni and Rayleigh problems have been carried out at the infinite Prandtl number limit, the linear theory results are of course valid for all Prandtl numbers. The Prandtl number limitation only affects the higher order results of the theory such as $(Ma)_1$, $(Ra)_2$, and the nonlinear solutions which will be presented later.

Acknowledgement—Partial support for R. Narayanan was provided by the Institute of Gas Technology.

REFERENCES

1. S. Chandrasekhar, *Hydrodynamic and Hydromagnetic Stability*. Clarendon Press, Oxford (1961).
2. E. L. Koschmieder, Bénard convection, *Adv. Chem. Phys.* **26,** 177–212 (1973).
3. E. Palm, Nonlinear thermal convection, *Ann. Rev. Fluid Mech.* **7,** 39–61 (1975).
4. R. H. Rogers, Convection, *Rep. Prog. Phys.* **39,** 1–63 (1976).
5. Lord Rayleigh, On convection currents in a horizontal layer of fluid when the higher temperature is on the under side, *Phil. Mag.* **32,** 529–546 (1916).
6. H. Jeffreys, The stability of a layer of fluid heated below, *Phil. Mag.* **2,** 833–844 (1926).
7. H. Jeffreys, Some cases of instability in fluid motion, *Proc. R. Soc.* **118A,** 195–208 (1928).
8. H. Jeffreys, The instability of a compressible fluid heated below, *Proc. Camb. Phil. Soc.* **26,** 170–172 (1930).
9. A. R. Low, On the criterion for stability of a layer of viscous fluid heated from below, *Proc. R. Soc.* **125A,** 180–195 (1929).
10. A. Pellew and R. V. Southwell, On maintained convective motion in a fluid heated from below, *Proc. R. Soc.* **176A,** 312–343 (1940).
11. W. H. Reid and D. L. Harris, Some further results on the Bénard problem, *Physics Fluids* **1,** 102–110 (1958).
12. J. R. A. Pearson, On convection cells induced by surface tension, *J. Fluid Mech.* **4,** 489–500 (1958).
13. L. E. Scriven and C. V. Sternling, On cellular convection driven by surface-tension gradients: effects of mean surface tension and surface viscosity, *J. Fluid Mech.* **19,** 321–340 (1964).
14. D. A. Nield, Surface tension and buoyancy effects in cellular convection, *J. Fluid Mech.* **19,** 341–352 (1964).
15. D. A. Nield, Streamlines in Bénard convection cells induced by surface tension and buoyancy, *Z. Angew. Math. Phys.* **17,** 226–232 (1966).
16. K. A. Smith, On convective instability induced by surface-tension gradients, *J. Fluid Mech.* **24,** 401–414 (1966).
17. J. C. Berg and A. Acrivos, The effect of surface active agents on convection cells induced by surface tension, *Chem. Engng Sci.* **20,** 737–745 (1965).
18. R. W. Zeren and W. C. Reynolds, Thermal instabilities in two-fluid horizontal layers, *J. Fluid Mech.* **53,** 305–327 (1972).
19. W. V. R. Malkus and G. Veronis, Finite amplitude cellular convection, *J. Fluid Mech.* **4,** 225–260 (1958).
20. A. Schlüter, D. Lortz and F. Busse, On the stability of steady finite amplitude convection, *J. Fluid Mech.* **23,** 129–144 (1965).
21. J. W. Scanlon and L. A. Segel, Finite amplitude cellular convection induced by surface tension, *J. Fluid Mech.* **30,** 149–162 (1967).
22. D. D. Joseph and C. C. Shir, Subcritical convective instability Part 1. Fluid layers, *J. Fluid Mech.* **26,** 753–768 (1966).
23. J. R. Kraska and R. L. Sani, Finite amplitude Bénard-Rayleigh convection, *Int. J. Heat Mass Transfer* **22,** 535–546 (1979).
24. D. D. Joseph, Stability of convection in containers of arbitrary shape, *J. Fluid Mech.* **47,** 257–282 (1971).
25. S. Ostrach and D. Pnueli, The thermal instability of completely confined fluids inside some particular configurations, *J. Heat Transfer* **85,** 346–354 (1963).
26. W. Velte, Stabilitätsverhalten und verzweigung stationärer lösungen der Navier-Stokesschen gleichungen, *Arch. Rat. Mech. Anal.* **16,** 97–125 (1964).
27. J. E. Fromm, Numerical solutions of the nonlinear equations for a heated fluid layer, *Physics Fluids* **8,** 1757–1769 (1965).
28. U. H. Kurzweg, Convective instability of a hydromagnetic fluid within a rectangular cavity, *Int. J. Heat Mass Transfer* **8,** 35–41 (1965).

29. M. Sherman and S. Ostrach, Lower bounds to the critical Rayleigh number in completely confined regions, *J. Appl. Mech.* **34,** 308–312 (1967).
30. M. R. Samuels and S. W. Churchill, Stability of a fluid in a rectangular region heated from below, *A.I.Ch.E. Jl* **13,** 77–85 (1967).
31. S. H. Davis, Convection in a box: linear theory, *J. Fluid Mech.* **30,** 465–478 (1967).
32. S. H. Davis, Convection in a box: on the dependence of preferred wave-number upon the Rayleigh number at finite amplitude, *J. Fluid Mech.* **32,** 619–624 (1968).
33. S. F. Liang, A. Vidal and A. Acrivos, Buoyancy-driven convection in cylindrical geometries, *J. Fluid Mech.* **36,** 239–256 (1969).
34. D. K. Edwards, Suppression of cellular convection by lateral walls, *J. Heat Transfer* **91,** 145–150 (1969).
35. I. Catton and D. K. Edwards, Initiation of thermal convection in finite right circular cylinders, *A.I.Ch.E. Jl* **16,** 594–601 (1970).
36. I. Catton, Convection in a closed rectangular region: the onset of motion, *J. Heat Transfer* **92,** 186–188 (1970).
37. I. Catton, The effect of insulating vertical walls on the onset of motion in a fluid heated from below, *Int. J. Heat Mass Transfer* **15,** 665–672 (1972).
38. G. S. Charlson and R. L. Sani, Thermoconvective instability in a bounded cylindrical fluid layer, *Int. J. Heat Mass Transfer* **13,** 1479–1496 (1970).
39. G. S. Charlson and R. L. Sani, On thermoconvective instability in a bounded cylindrical fluid layer, *Int. J. Heat Mass Transfer* **14,** 2157–2160 (1971).
40. P. A. Jennings and R. L. Sani, Some remarks on thermoconvective instability in completely confined regions, *J. Heat Transfer* **94,** 234–236 (1972).
41. G. S. Charlson and R. L. Sani, Finite amplitude axisymmetric thermoconvective flows in a bounded cylindrical layer of fluid, *J. Fluid Mech.* **71,** 209–229 (1975).
42. R. P. Davies-Jones, Thermal convection in an infinite channel with no-slip sidewalls, *J. Fluid Mech.* **44,** 695–704 (1970).
43. C. A. Jonès, D. R. Moore and N. O. Weiss, Axisymmetric convection in a cylinder, *J. Fluid Mech.* **73,** 353–388 (1976).
44. E. L. Koschmieder, On convection under an air surface, *J. Fluid Mech.* **30,** 9–15 (1967).
45. C. Q. Hoard, C. R. Robertson and A. Acrivos, Experiments on the cellular structure in Bénard convection, *Int. J. Heat Mass Transfer* **13,** 849–856 (1970).
46. H. J. Palmer and J. C. Berg, Convective instability in liquid pools heated from below, *J. Fluid Mech.* **47,** 779–787 (1971).
47. H. Bénard, Les tourbillons cellulaires dans une nappe liquide transportant de la chaleur par convection en regime permanent, *Ann. Chem. Phys.* **23,** 62–144 (1901).
48. J. L. Duda and J. S. Vrentas, Steady flow in the region of closed streamlines in a cylindrical cavity, *J. Fluid Mech.* **45,** 247–260 (1971).
49. S. S. Agrawal, Nonlinear free surface convection in a bounded cylindrical geometry, Ph.D. Thesis, Illinois Institute of Technology (1980).
50. A. Vidal and A. Acrivos, Nature of the neutral state in surface-tension driven convection, *Physics Fluids* **9,** 615–616 (1966).
51. I. Stakgold, *Green's Functions and Boundary Value Problems.* John Wiley, New York (1979).
52. K. Kirchgässner and P. Sorger, Branching analysis for the Taylor problem, *Quart. J. Mech. Appl. Math.* **22,** 183–209 (1969).
53. R. Narayanan, Free surface convection in cylindrical geometries, Ph.D. Thesis, Illinois Institute of Technology (1978).
54. M. Bentwich, Buoyancy and surface-tension induced instabilities of fluid in open and closed vertical cylindrical containers, *Appl. Sci. Res.* **24,** 305–328 (1971).
55. S. H. Davis, Buoyancy-surface tension instability by the method of energy, *J. Fluid Mech.* **39,** 347–359 (1969).

CONVECTION DE SURFACE LIBRE DANS UNE GEOMETRIE A FRONTIERE CYLINDRIQUE

Résumé—On étudie la convection provoquée par la tension interfaciale et la convection naturelle dans une géométrie à frontière cylindrique, avec une surface libre, pour différentes valeurs du rapport de forme et du nombre de Nusselt. La théorie linéaire et quelques aspects de l'analyse non-linéaire sont utilisés pour déterminer les nombres critiques de Marangoni et de Rayleigh, la structure du mouvement convectif, la direction de l'écoulement et la nature des bifurcations. L'analyse est basée sur une méthode particulière de traitement des problèmes de convection, par utilisation des fonctions de Green pour réduire le problème à la résolution d'une équation intégrale.

KONVEKTION AN EINER FREIEN OBERFLÄCHE IN EINEM ZYLINDRISCH BEGRENZTEN GEBIET

Zusammenfassung—Es wurde die durch Oberflächenspannung und Auftriebskräfte verursachte Konvektion in einem zylindrisch begrenzten Gebiet mit freier Oberfläche für eine Reihe von Seitenverhältnissen und Nusselt-Zahlen untersucht. Die lineare Theorie und einige Gesichtspunkte der nichtlinearen Analysis werden dazu benutzt, die kritischen Marangoni- und Rayleigh-Zahlen, die Struktur der konvektiven Bewegung, die Strömungsrichtung und den Vorgang der gabelartigen Verzweigung zu bestimmen. Die Analysis stützt sich auf eine bei der Behandlung von Problemen der freien Konvektion etwas unübliche Methode, nämlich die Anwendung der Green'schen Funktionen zur Reduzierung des Problems auf die Lösung einer Integralgleichung.

СВОБОДНАЯ КОНВЕКЦИЯ ОТ ПОВЕРХНОСТИ В ОГРАНИЧЕННОМ ЦИЛИНДРИЧЕСКОМ ПРОСТРАНСТВЕ

Аннотация — Исследуется конвекция, вызываемая силами поверхностного натяжения и подъемными силами, в ограниченном цилиндрическом пространстве при различных отношениях сторон и значениях числа Нуссельта. Для определения критических чисел Марангони и Релея, структуры конвективного потока, направления течения и природы бифуркации применяется линейный анализ и некоторые аспекты нелинейного анализа. Используется несколько модифицированный метод решения задач свободной конвекции, а также функция Грина для сведения задачи к интегральному уравнению.